Sensitivity of a DC SQUID with a non-sinusoidal current-phase relation in its junctions

J. R. Prance[1] and M. D. Thompson[1]

Department of Physics, Lancaster University, Lancaster, LA1 4YB, UK

(*Electronic mail: j.prance@lancaster.ac.uk)

(Dated: 12 May 2023)

In ballistic SNS Josephson junctions, such as those made from graphene or high mobility semiconductors, the current-phase relation may not have the common, sinusoidal form but can be skewed to have a peak supercurrent at a phase difference greater than $\pi/2$. Here we use a numerical simulation that includes thermal noise to investigate the sensitivity of a DC SQUID with such junctions. The simulation uses an RCSJ model where the current-phase relation of each junction can be defined as an arbitrary function. The modulation, transfer function, noise and sensitivity of a SQUID are calculated for different types of current-phase relation. For the examples considered here, we find that the flux sensitivity of the SQUID is always degraded by forward skewing of the current-phase relation, even in cases where the transfer function of the SQUID has been improved.

The current-phase relation (CPR) of superconducting junctions can take many forms that are different to the typical, sinusoidal relation originally associated with the DC Josephson effect[1]. Here we study numerically the sensitivity of a DC SQUID where the Josephson junctions have non-sinusoidal CPRs that are skewed to give a peak supercurrent at a phase difference greater than $\pi/2$. CPRs of this form can occur in highly ballistic SNS junctions such as those made from graphene or high mobility semiconductors, as predicted by theory[1–6] and observed in experiments[7–19].

The effect of non-sinusoidal CPRs in the junctions of a DC SQUID has previously been considered with respect to the modulation of switching current with applied magnetic flux in the absence of noise[20,21]. Similar models have been applied to graphene-based DC SQUIDs[11]. Work on micro- and nano-SQUIDs has gone further to predict the finite voltage above the switching current for some non-sinusoidal CPRs in the presence of noise[22]. This last work contains the information needed to quantify SQUID sensitivity, but not for the CPRs or the range of parameters considered here. In this work, we use a resistively and capacatively shunted junction (RCSJ) model to predict important properties of a DC SQUID that contains junctions with various different forms of CPR. The formulation of the model is familiar from the literature, as summarised in *The SQUID Handbook*[23], and it has been shown that the RCSJ model can provide a good description of the dynamics of individual graphene junctions[24].

We follow the approach of Tesche and Clarke[23,25] to implement a numerical simulation of the RCSJ model in the presence of thermal noise. In our model, the sinusoidal CPR is replaced with an arbitrary function $i_{\mathrm{SC}}(\delta)$, where δ is the superconducting phase difference across a junction and $\max(i_{\mathrm{SC}}) = 1$. Further details of how the model is implemented can be found in the supplementary material and the code is available[26].

Figure 1(a) and Fig. 1(b) show examples of the calculated, time-averaged DC voltage $\langle v \rangle$ across two SQUIDs as a function of applied flux ϕ_a and DC current i. All three quantities are expressed as dimensionless values. Currents are normalised by the average critical current of the junctions I_0. Voltages are normalised by I_0R where R is twice the parallel resistance of the two junctions in the normal state. The flux ϕ_{a} is the applied magnetic flux in units of the magnetic flux quantum. Using standard definitions[23], the SQUID is characterised by its Stewart-McCumber parameter β_c, normalised loop inductance β_L and four parameters that defined the asymmetry of the critical currents α_I, junction shunt resistances α_R, junction capacitances α_C, and the inductances on each side of the SQUID loop α_L.

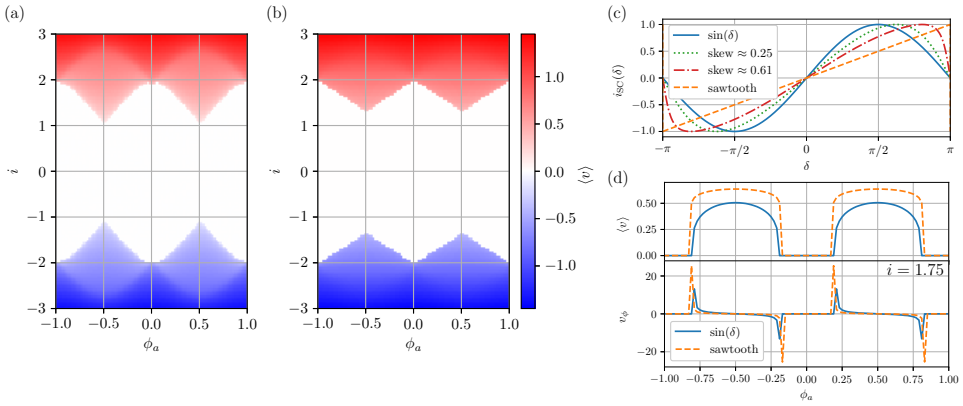

FIG. 1. Numerical simulation of the time-averaged voltage $\langle v \rangle$ across two symmetric SQUIDs ($\alpha_I = \alpha_R = \alpha_C = \alpha_L = 0$) with $\beta_c = 1.0$, $\beta_L = 1.0$. In (a) the SQUID junctions have a sinusoidal CPR and in (b) the junctions have a sawtooth CPR. Both CPRs are shown in (c) together with two intermediate, forward-skewed examples. These are calculated using Eq. 1 with $T = 0.80$ to produce a skew of 0.25 and $T = 0.99$ to produce a skew of 0.61. (d) Shows voltage and the transfer function $v_\phi = d\langle v \rangle / d\phi_a$ as a function of flux for both SQUIDs at a current $i = 1.75$.

Figure 1(a) shows the calculated voltage across a SQUID whose junctions have a sinusoidal CPR while Fig. 1(b) is for a SQUID whose junctions have a highly-skewed, sawtooth CPR. The form of the CPRs clearly has a significant influence on the modulation of both the switching current i_s and the average voltage $\langle v \rangle$ as a function of flux. The shape of the CPR therefore affects the response of the SQUID to changes in flux as quantified by the transfer function $v_\phi = d\langle v \rangle / d\phi_a$.

Fig. 1(d) shows that the sawtooth CPR generally reduces the transfer function, as compared to a sinusoidal case, except at the switching current where transitions from finite $\langle v \rangle$ to $\langle v \rangle = 0$ are sharper. The main motivation for this work is to determine whether the large transfer functions that occur at these sharp features can be used to achieve better overall sensitivity when thermal noise is taken into account.

The sawtooth CPR used to calculate Fig. 1(b) applies to the extreme case of a uniform and perfectly ballistic junction at low temperature. In practice, the CPR of an SNS junction at finite temperature with high, but not perfect, transmission and imperfect contacts is likely to be intermediate between a sawtooth and sine[2–12,16,18], with maximum supercurrent at a phase in the range

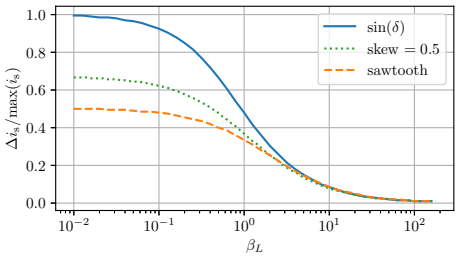

FIG. 2. Depth of modulation of the SQUID switching current $i_s(\phi_a)$ across a range of β_L, from numerical simulations using the three different CPRs. The junction capacitance is $\beta_c = 0.1$. At low β_L, the sawtooth CPR halves the modulation depth of i_s compared to the sinusoidal CPR.

$\pi/2 < \delta < \pi$. Two examples are shown in Fig. 1(c). They are calculated using equation 1, which applies to short SNS junctions with a single conducting channel of transmission probability T, in the limit of low temperatures (Ref. 1).

$$i_{SC}(\delta) \propto \frac{T\sin(\delta)}{\sqrt{1 - T\sin^2(\delta/2)}} \tag{1}$$

We use equation 1 to produce forward-skewed CPRs in the simulations not because it is strictly correct for every type of junction that might be of interest but because it is a relatively efficient way to implement a smooth, forward-skewed function. When such a CPR is used in this work it is characterised by the 'skew', defined as the position of the maximum supercurrent with respect to $\delta = \pi/2$, as a fraction of $\pi/2$.

Figure 2 shows in detail how the modulation with flux of the switching current of a SQUID is affected by the CPR of its junctions. As expected, the modulation is reduced when the junctions have a forward-skewed CPR[20,21,27,28]. For a symmetric SQUID with negligible loop inductance ($\beta_L \ll 1$) and junctions with a sinusoidal CPR, the switching current is fully suppressed at $\phi_a = (n + \frac{1}{2})$, where n is an integer, giving a modulation depth of $\Delta i_s/\max(i_s) = 1$. If instead the SQUID junctions have a sawtooth CPR then $i_s \geq 1.0$ for all ϕ_a and the maximum possible modulation depth is $\Delta i_s/\max(i_s) = 0.5$. The modulation depth for all three CPRs shown in Fig. 2 converge for $\beta_L \gg 1$.

For a typical SQUID with sinusoidal CPR in its junctions, the scaling with β_L of the modulation depth of the switching current is similar to the scaling of the maximum transfer function: the transfer function is largest for $\beta_L \ll 1$ and tends to zero for $\beta_L \gg 1$. The same is true for junctions

with a highly skewed CPR, but the sharp features that occur close to the switching current [(see Fig. 1(d)] can produce much larger transfer functions at low β_L. In a simulation with no noise, the sawtooth CPR can produce an arbitrarily large transfer function. To understand how this affects the sensitivity, it is necessary to also consider the noise of the SQUID at these particular points.

To introduce intrinsic noise into the model, two random current sources are added in parallel to the junctions to represent Johnson noise in their shunt resistances. The noise currents i_{N1} and i_{N2} have a dimensionless power spectral density $s_i = 4\Gamma$. The value of Γ can be interpreted in several ways, including as the ratio of the thermal energy to the Josephson energy, $\Gamma = k_{\mathrm{B}}T/E_{\mathrm{J}}$[23]. In practice, the numerical simulation randomises the values of i_{N1} and i_{N2} every τ_{N} units of time (typically, $\tau_{\mathrm{N}} = 0.1$). The correct spectral density is obtained by choosing random numbers from a normal distribution of width $\sqrt{2\Gamma/\tau_{\mathrm{N}}}$. Here we use the dimensionless time $\tau = (2eI_0R/\hbar)t$.

The random currents drive the SQUID in a way that depends on its static parameters and its instantaneous state. In general, the addition of noise has the effect of smoothing out sharp features in $\langle v \rangle$ as a function of i and ϕ_a (see supplementary material for more details). This reduces the transfer function. The noise currents also generate voltage noise across the SQUID, which is generally larger for larger Γ but also depends on i and ϕ_a.

The sensitivity of a SQUID to magnetic flux is determined by both its transfer function and its voltage noise. The transfer function quantifies the conversion of flux to DC voltage, $V_\Phi = dV/d\Phi_a$, and the minimum detectable flux is limited by the voltage noise, characterised by its power spectral density S_{V}. The flux sensitivity, expressed as a flux noise power spectral density, is $S_\Phi = S_{\mathrm{V}}/V_\Phi^2$. In our simulations, the dimensionless transfer function $v_\phi = V_\Phi\Phi_0/I_0R = d\langle v \rangle/d\phi_a$ is found by numerically differentiating calculated values of $\langle v \rangle$. The dimensionless voltage noise $s_v = S_{\mathrm{V}}(2\pi/I_0R\Phi_0)$ is found from the low-frequency power spectral density of simulated time series $v(\tau)$. (Power spectral densities are calculated using the SciPy library function '`scipy.signal.welch`'[29]. An example time series and power spectrum can be found in the supplementary material.) These quantities give the dimensionless flux sensitivity $s_\phi = S_\Phi(2\pi I_0R/\Phi_0^3) = s_v/v_\phi^2$. The noise currents i_{N1} and i_{N2} affect both components of the sensitivity, v_ϕ and s_v. In general, the sensitivity gets worse (s_ϕ increases) as the noise increases.

Figure 3 compares the sensitivity of two SQUIDs that have identical parameters but different CPRs. For a symmetric SQUID ($\alpha_I = \alpha_R = \alpha_C = \alpha_L = 0$) the best sensitivity is typically found at $\phi_a \approx 0.25$ and $i \gtrsim i_{\mathrm{s}}$[23]. To find the best sensitivity we combine the transfer function $v_\phi(i)$ with the simulated voltage noise $s_v(i)$ at $\phi_a = 0.25$. The best sensitivity is the miniumum value of

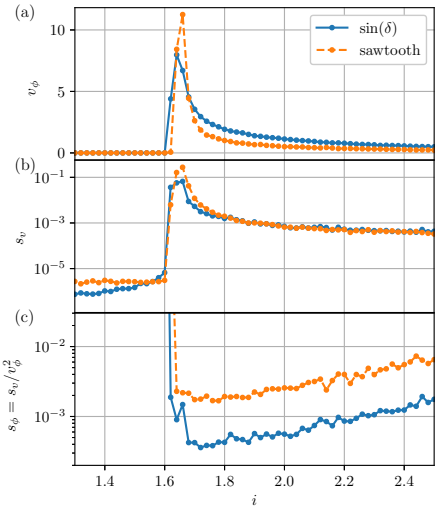

FIG. 3. Flux sensitivity s_ϕ determined by simulation of two symmetric SQUIDs, each with a different CPR in its junctions. Noise is included with $\Gamma = 10^{-4}$ and $\beta_L = 1$, $\beta_C = 0.1$. The voltage $v(\tau)$ across each SQUID is simulated for 10^4 time units, with $2.5 > i > i_s(\phi_a)$ and for a small range of ϕ_a about $\phi_a = 0.25$. (a) shows the transfer function $v_\phi = d\langle v\rangle / d\phi_a$ as a function of i at $\phi_a = 0.25$, found by numerical differentiation of the time-averaged voltage. (b) shows the low frequency spectral density of the simulated voltage time series $v(\tau)$. (c) shows the resulting flux sensivity $s_\phi = s_v/v_\phi^2$.

$s_\phi = s_v(i)/v_\phi(i)^2$.

For the examples shown in Fig. 3, the noise is sufficiently low that the sawtooth CPR produces a large peak in v_ϕ, close to the switching current. This corresponds to a sharp transition of the type shown in Fig. 1(c). However, as shown in Fig. 3(b), the noise is also larger at the point where the transfer function is large. The net effect is higher s_ϕ (worse sensitivity) than for the sinusoidal CPR. At higher i, the noise is similar for the two cases but the sawtooth CPR results in a consistently lower transfer function. Again, the result is that the sinusoidal CPR produces better sensitivity (lower s_ϕ). Overall, for this choice of parameters the sinusoidal CPR produces better sensitivity across all i.

Figure 4 shows the best sensitivity for SQUIDs with a range of loop inductances β_L and thermal noise Γ. It also includes results for an intermediate CPR with a skewness of 0.5. In all cases, the flux sensitivity is either unaffected or degraded by forward-skewing of the CPR. For the majority

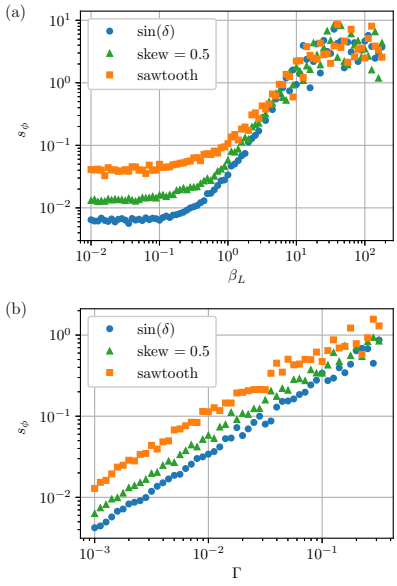

FIG. 4. Simulated flux sensitivity of symmetric DC SQUIDs with $\beta_c = 0.1$. (a) shows flux sensitivity as a function of normalised loop inductance β_L. Good sensitivity (flux noise power $s_\phi \ll 1$) is obtained for $\beta_L \lesssim 1$. In this range, junctions with a sinusoidal CPR always produce better sensitivity (lower s_ϕ) than junctions with a sawtooth CPR. Thermal noise is included with $\Gamma = 0.01$. (b) shows flux sensitivity as a function of thermal noise for $\beta_L = 1$. As expected, sensitivity improves with decreasing thermal noise. Junctions with sinusoidal CPR produce better sensitivity across the whole range. The results in (a) and (b) are obtained by simulating the voltage across each SQUID for 4×10^4 time units at every point.

of the results shown in Fig. 4, the sensitivity is worse than the sinusoidal case because the transfer function is lower at the point of best sensitivity. However, as shown in Fig. 3, the sensitivity is not improved even when the transfer function is higher because of an associated increase in voltage noise.

In conclusion, numerical simulations using a modified RCSJ model show that forward skewing of the CPRs in a DC SQUID results in poorer flux sensitivity across a wide range of parameters. While skewing of the CPR produces a stronger intrinsic response to the phase difference across a single junction (a larger maximum $di_{SC}/d\delta$) this does not translate into better sensitivity when two junctions form a DC SQUID. At the particular operating points where forward skewing can

increase the transfer function, the voltage noise is also larger, resulting in an overall degradation of sensitivity.

SUPPLEMENTARY MATERIAL

See the supplementary material for additional details of the numerical simulation used in this work.

ACKNOWLEDGMENTS

This project has received funding from the European Union's Horizon 2020 research and innovation program under Grant Agreements No 881603 and 824109. Results were calculated using The High End Computing facility at Lancaster University. M.D.T acknowledges financial support from the Royal Academy of Engineering (RF\201819\18\2). The authors would like to thank Richard Haley for helpful discussions.

AUTHOR DECLARATIONS

Conflict of Interest

The authors have no conflicts to disclose

Author Contributions

J. R. Prance: Investigation (equal); Conceptualization (equal); Writing, review and editing (equal); Software (lead) **M. D. Thompson:** Investigation (equal); Conceptualization (equal); Writing, review and editing (equal); Software (supporting)

DATA AVAILABILITY STATEMENT

The data and code that support the findings of this study are openly available at reference number 26, https://dx.doi.org/10.17635/lancaster/researchdata/592.

REFERENCES

[1]A. A. Golubov, M. Y. Kupriyanov, and E. Il'ichev, "The current-phase relation in josephson junctions," Rev. Mod. Phys. **76**, 411–469 (2004).

[2]A. M. Black-Schaffer and S. Doniach, "Self-consistent solution for proximity effect and josephson current in ballistic graphene SNS josephson junctions," Phys. Rev. B **78**, 024504 (2008).

[3]A. M. Black-Schaffer and J. Linder, "Strongly anharmonic current-phase relation in ballistic graphene josephson junctions," Phys. Rev. B **82**, 184522 (2010).

[4]I. Hagymási, A. Kormányos, and J. Cserti, "Josephson current in ballistic superconductor-graphene systems," Phys. Rev. B **82**, 134516 (2010).

[5]H. Meier, V. I. Fal'ko, and L. I. Glazman, "Edge effects in the magnetic interference pattern of a ballistic SNS junction," Phys. Rev. B **93**, 184506 (2016).

[6]P. Rakyta, A. Kormányos, and J. Cserti, "Magnetic field oscillations of the critical current in long ballistic graphene josephson junctions," Phys. Rev. B **93**, 224510 (2016).

[7]C. Girit, V. Bouchiat, O. Naaman, Y. Zhang, M. F. Crommie, A. Zettl, and I. Siddiqi, "Current-phase relation in graphene and application to a superconducting quantum interference device," Physica Status Solidi (b) **246**, 2568–2571 (2009).

[8]G.-H. Lee, S. Kim, S.-H. Jhi, and H.-J. Lee, "Ultimately short ballistic vertical graphene josephson junctions," Nature Communications **6**, 6181 (2015).

[9]C. D. English, D. R. Hamilton, C. Chialvo, I. C. Moraru, N. Mason, and D. J. Van Harlingen, "Observation of nonsinusoidal current-phase relation in graphene josephson junctions," Phys. Rev. B **94**, 115435 (2016).

[10]M. D. Thompson, M. B. Shalom, A. K. Geim, A. J. Matthews, J. White, Z. Melhem, Y. A. Pashkin, R. P. Haley, and J. R. Prance, "Graphene-based tunable squids," Applied Physics Letters **110**, 162602 (2017).

[11]G. Nanda, J. L. Aguilera-Servin, P. Rakyta, A. Kormányos, R. Kleiner, D. Koelle, K. Watanabe, T. Taniguchi, L. M. K. Vandersypen, and S. Goswami, "Current-phase relation of ballistic graphene josephson junctions," Nano Letters **17**, 3396–3401 (2017).

[12]E. M. Spanton, M. Deng, S. Vaitiekėnas, P. Krogstrup, J. Nygård, C. M. Marcus, and K. A. Moler, "Current-phase relations of few-mode InAs nanowire josephson junctions," Nat. Phys. **13**, 1177 (2017).

[13]A. Murani, A. Kasumov, S. Sengupta, Y. A. Kasumov, V. T. Volkov, I. I. Khodos, F. Brisset, R. Delagrange, A. Chepelianskii, R. Deblock, H. Bouchiat, and S. Guéron, "Ballistic edge states in bismuth nanowires revealed by squid interferometry," Nature Communications **8**, 15941 (2017).

[14]F. E. Schmidt, M. D. Jenkins, K. Watanabe, T. Taniguchi, and G. A. Steele, "A ballistic graphene superconducting microwave circuit," Nat. Commun. **9**, 4069 (2018).

[15]S. Hart, Z. Cui, G. Ménard, M. Deng, A. E. Antipov, R. M. Lutchyn, P. Krogstrup, C. M. Marcus, and K. A. Moler, "Current-phase relations of InAs nanowire josephson junctions: From interacting to multimode regimes," Phys. Rev. B **100**, 064523 (2019).

[16]M. Kayyalha, A. Kazakov, I. Miotkowski, S. Khlebnikov, L. P. Rokhinson, and Y. P. Chen, "Highly skewed current-phase relation in superconductor-topological insulator-superconductor josephson junctions," npj Quantum Materials **5**, 7 (2020).

[17]F. M. D. Pellegrino, G. Falci, and E. Paladino, "1/f critical current noise in short ballistic graphene josephson junctions," Communications Physics **3**, 6 (2020).

[18]W. Mayer, M. C. Dartiailh, J. Yuan, K. S. Wickramasinghe, E. Rossi, and J. Shabani, "Gate controlled anomalous phase shift in Al/InAs josephson junctions," Nature Communications **11**, 212 (2020).

[19]P. Zhang, A. Zarassi, L. Jarjat, V. Van de Sande, M. Pendharkar, J. S. Lee, C. P. Dempsey, A. P. McFadden, S. D. Harrington, J. T. Dong, H. Wu, A. H. Chen, M. Hocevar, C. J. Palmstrøm, and S. M. Frolov, "Large Second-Order Josephson Effect in Planar Superconductor-Semiconductor Junctions," arXiv e-prints , arXiv:2211.07119 (2022), arXiv:2211.07119 [cond-mat.mes-hall].

[20]T. A. Fulton, L. N. Dunkleberger, and R. C. Dynes, "Quantum interference properties of double josephson junctions," Phys. Rev. B **6**, 855–875 (1972).

[21]W.-T. Tsang and T. Van Duzer, "Influence of the current-phase relation on the critical-current-applied-magnetic-flux dependence in parallel-connected josephson junctions," Journal of Applied Physics **47**, 2656–2661 (1976).

[22]C. Granata, A. Vettoliere, M. Russo, and B. Ruggiero, "Noise theory of dc nano-SQUIDs based on dayem nanobridges," Phys. Rev. B **84**, 224516 (2011).

[23]J. Clarke and A. I. Braginski, eds., *The SQUID Handbook*, Vol. 1: Fundamentals and Technology of SQUIDs and SQUID Systems (Wiley-VCH Verlag, 2006).

[24]T. F. Q. Larson, L. Zhao, E. G. Arnault, M.-T. Wei, A. Seredinski, H. Li, K. Watanabe, T. Taniguchi, F. Amet, and G. Finkelstein, "Zero crossing steps and anomalous shapiro maps in

graphene josephson junctions," Nano Letters **20**, 6998–7003 (2020).

[25]C. D. Tesche and J. Clarke, "DC SQUID: Noise and optimization," Journal of Low Temperature Physics **29**, 301–331 (1977).

[26]J. R. Prance and M. D. Thompson, "Simulation of DC SQUIDs using an RCSJ model," https://dx.doi.org/10.17635/lancaster/researchdata/592 (2023).

[27]K. Hasselbach, D. Mailly, and J. R. Kirtley, "Micro-superconducting quantum interference device characteristics," Journal of Applied Physics **91**, 4432–4437 (2002).

[28]G. J. Podd, G. D. Hutchinson, D. A. Williams, and D. G. Hasko, "Micro-SQUIDs with controllable asymmetry via hot-phonon controlled junctions," Phys. Rev. B **75**, 134501 (2007).

[29]P. Virtanen, R. Gommers, T. E. Oliphant, M. Haberland, T. Reddy, D. Cournapeau, E. Burovski, P. Peterson, W. Weckesser, et al., and SciPy 1.0 Contributors, "SciPy 1.0: Fundamental Algorithms for Scientific Computing in Python," Nature Methods **17**, 261–272 (2020).

[30]F. Auracher and T. Van Duzer, "Influence of the current-phase relationship on the i-v characteristic of superconducting weak links," Applied Physics Letters **21**, 515–518 (1972).

[31]C. Girit, V. Bouchiat, O. Naaman, Y. Zhang, M. F. Crommie, A. Zettl, and I. Siddiqi, "Tunable graphene dc superconducting quantum interference device," Nano Letters **9**, 198–199 (2009).

[32]K. Tsumura, M. Ohsugi, T. Hayashi, E. Watanabe, D. Tsuya, S. Nomura, and H. Takayanagi, "Development of superconducting interference device based on graphene," Journal of Physics: Conference Series **400**, 042064 (2012).

[33]M. Titov and C. W. J. Beenakker, "Josephson effect in ballistic graphene," Phys. Rev. B **74**, 041401 (2006).

[34]S. M. Kogan and K. E. Nagaev, "Fluctuation kinetics in superconductors at frequencies low compared with the energy gap," J. Exp. Theor. Phys. **67**, 579 (1988).

[35]I. N. Askerzade, "Effects of anharmonicity of current-phase relation in josephson junctions (review article)," Low Temperature Physics **41**, 241–259 (2015).

Applied Physics Letters

PLEASE CITE THIS ARTICLE AS DOI: 10.1063/5.0151607

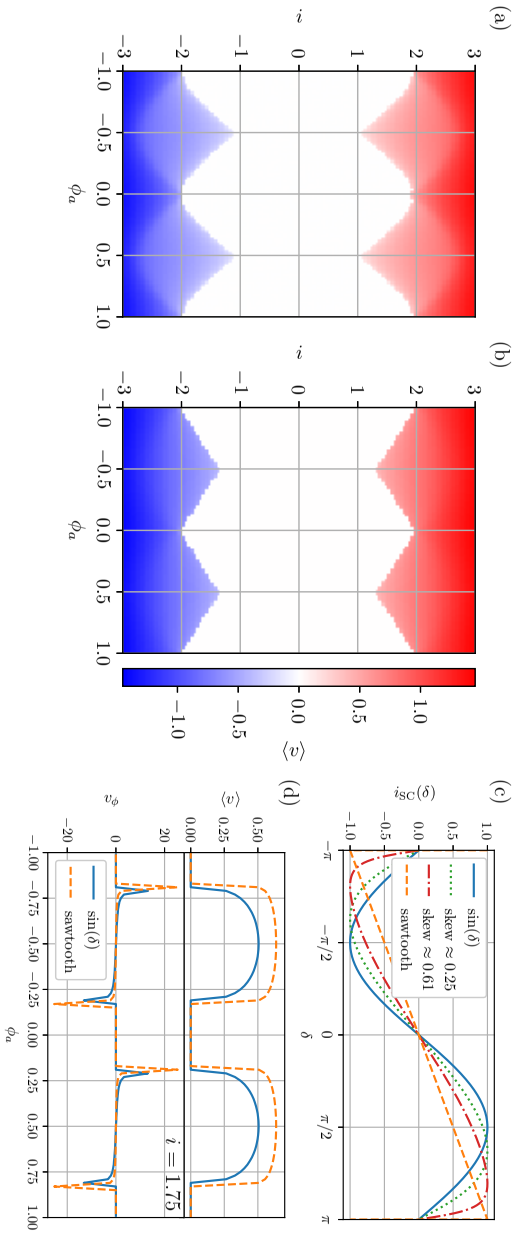

Applied Physics Letters

PLEASE CITE THIS ARTICLE AS DOI: 10.1063/5.0151607